

MULTIPLICITY-CORRECTED MASS FUNCTION OF MAIN-SEQUENCE STARS IN THE SOLAR NEIGHBORHOOD

SARBANI BASU

Tata Institute of Fundamental Research, Homi Bhabha Road, Bombay-400 005, India

AND

N. C. RANA¹

Inter-University Center for Astronomy and Astrophysics, Post Bag No. 4, Ganeshkhind, Pune-411 007, India

Received 1991 May 29; accepted 1992 January 7

ABSTRACT

The present-day mass function (PDMF) of stars in the solar neighborhood has been derived after correcting the photometric luminosity function for the effects of unresolved multiple stellar systems. Such a PDMF gives a stellar surface mass density of $39.5 M_{\odot} \text{ pc}^{-2}$ as opposed to only $31.3 M_{\odot} \text{ pc}^{-2}$ given by the PDMF not corrected for the effects of stellar multiplicity. We have also calculated the initial mass function (IMF) of stars from the corrected PDMF using a number of star-formation rates with exponential time dependence—a form which gives good fits to data on chemical evolution. We find that the neutron star and white dwarf formation rates restrict the reciprocal of the time constant of star formation to the range between -0.1 and $+0.1 \text{ Gyr}^{-1}$. The IMF for stellar masses greater than $1.4 M_{\odot}$ can be represented as a power law with an exponent of -1.56 ± 0.05 . However, for masses greater than $6.5 M_{\odot}$, a power of -1.67 fits better. The ratio of the mass of gas returned to the ISM by the stars to the total mass of gas that has ever gone into star formation—the returned fraction—is found to be a rapidly increasing function of the reciprocal of the time constant of star formation. The fraction of remnants and evolved stars also show the same trend, but the increase is not as rapid. The total surface mass density predicted by the IMF is consistent with the presence of very little or no nonbaryonic dark matter in the Galactic disk in the solar neighborhood.

Subject headings: binaries: general — stars: luminosity function, mass function — stars: statistics

1. INTRODUCTION

The frequency distribution of stars according to their masses, i.e., the mass-spectrum, is an important function in the study of Galactic chemical evolution. It is generally expressed as the number of stars present today per unit area of the disk per unit interval of the logarithm of the mass (the present-day mass function, or the PDMF), or more often as the total number of stars formed throughout the life of the Galactic disk per unit area per unit interval of logarithmic mass (the initial mass function, or the IMF). These two functions, in conjunction with other factors like the lifetime of stars, the products of stellar nucleosynthesis, etc., can indicate the number of stars which have died, the amount of gas and heavy elements ejected by them, the dark remnants they leave behind, etc.

There have been numerous attempts at deriving the PDMF and the IMF from observations (Miller & Scalo 1979; Garmany, Conti, & Chiosi 1982; Bisiacchi, Firmani, & Samiento 1983; Scalo 1986; Larson 1986; Rana 1987, 1990a, b, 1991) ever since Salpeter (1955) first studied the high-mass end of the IMF. The derivation of the PDMF and the IMF from the more directly observed luminosity function (LF) requires a number of other inputs from observations and simulations. In view of recent additions to the observational data used in determining the PDMF, and new simulations of stellar evolution, we update the PDMF given in Rana (1990a). While doing so we also try and apply a correction for a crucial factor which changes the total number of stars by a reasonably large factor, namely the multiplicity of stars.

The derivation of the PDMF uses the luminosity function of stars as the basic input. Most of the luminosity functions which have been determined are defined photometrically (Reid & Gilmore 1982; Gilmore, Reid, & Hewett 1985; Stobie, Ishida, & Peacock 1989, etc.). For stars near the Sun it has been seen that a photometrically defined luminosity function counts all stellar components of a multiple system as one object, i.e., a photometrically defined luminosity function is a system luminosity function rather than a stellar luminosity function (Stobie et al. 1989). The number of multiple systems in the solar neighborhood is believed to be quite large. Abt & Levy (1976) give the ratio of single stars, binaries, triple systems, and quadruple systems as 42:46:9:2. Halbwachs (1986) estimates that the proportion of single stars among all stellar systems is at most 23%. More recently Duquennoy (1988) gives the ratio of single stars, binaries, triple, and quadruple systems as 51:39:8:2, that is, a photometric survey would count only 100 stars instead of the 161 stars present. Some extreme estimates put the number of single field stars even lower (only about 5% according to Poveda 1988). Thus it becomes imperative to correct the PDMF for the effects of multiplicity. A failure to do so would result in an underestimation of the number of stars present today, and also of the total number of stars formed since the birth of the disk. It would also result, although indirectly, in an overestimation of nonbaryonic dark matter, if any, in the disk.

A preliminary effort to correct the PDMF for the effects of multiplicity was made by Pisunov & Malkov (1987). They concentrated on the very low-luminosity end of the luminosity function, and study the effects of the evolution of brown dwarfs. Another attempt was made by Rana (1990a), where he assumed that all the stellar components of a multiple system

¹ On leave from Tata Institute of Fundamental Research, Homi Bhabha Road, Bombay-400 005, India.

have equal masses, and that there is no need to correct the mass-luminosity calibration for the effects of multiplicity while determining the mass corresponding to any luminosity in using the luminosity function. We try to do a more detailed work here. We do not consider the very faint stars since data on them are very uncertain. In § 2, we outline the procedure to derive the PDMF and the IMF, and also discuss the observational inputs that are needed. We present and discuss the results in § 3. Conclusions are drawn in § 4.

2. PROCEDURE FOR DERIVING THE PDMF AND IMF AND THE OBSERVATIONAL INPUTS

The PDMF is given by (Miller & Scalo 1979)

$$\phi_{\text{ms}}(\log m) = \phi_{\text{LF}}(M_V) \left| \frac{dM_V}{d \log m} \right| 2 \langle H \rangle (M_V), \quad (1)$$

while the IMF, $\xi(\log m)$, can be written as

$$\xi(\log m) = E(m) \phi_{\text{ms}}(\log m), \quad (2)$$

where

$$E(m) = 1, \quad \text{for } m \leq m_t, \\ = \int_0^{t_d} \psi_s(t) dt / \int_{t_d - t_{\text{ms}}}^{t_d} \psi_s(t) dt, \quad \text{for } m > m_t. \quad (3)$$

In both equations m is the mass in solar mass units, and the subscript ms denotes the fact that we are dealing with main-sequence stars. $\phi_{\text{LF}}(M_V)$ is the luminosity function, that is, the number of stars per unit volume, which have an absolute V -magnitude in the range $M_V \pm 0.5$, and $\langle H \rangle$ is the mean scale height of the stars. The luminosity function is assumed to have been corrected for the fraction of stars which have evolved beyond the main sequence. The details of the correction can be found in Scalo (1986). In equation (3), $\psi_s(t)$ is the star-formation rate, t_{ms} the main-sequence lifetime of a star of mass

m , and m_t , is the mass for which $t_{\text{ms}} = t_d$. We discuss the main observational inputs to the PDMF and IMF below.

2.1. The m - M_V Relation

The mass corresponding to a given luminosity generally found by using binary star data. We have used the compilations of Popper (1980), along with those of Cester, Ferluga, & Boehm et al. (1983), Grenier et al. (1985), and Liebert & Probst (1987).

Figure 1a shows the result of binning the m - M_V data in bins of 0.1 in $\log m$. The same figure also shows the m - M_V relation adopted for this work. The low mass end of the m - M_V relation is uncertain with a large scatter. The flattening of the m - M_V relation around $0.5 M_\odot$, and the steepening thereafter for lower masses is expected on theoretical grounds (D'Antona 1990). The trend for the intermediate mass range is reasonably clear with not much scatter in the data.

If an observed object is not a single star but a multiple system, the use of the single star m - M_V relation will result in assigning it a mass larger than the mass of its primary star. This will manifest as a spurious increase in the number of stars toward the higher mass ranges giving an erroneous mass dependence of the PDMF and the IMF. Therefore in order to find the correct primary star mass corresponding to a given M_V bin, we have to construct the m - M_V relation appropriate for the multiple system, and use this "composite" m - M_V relation to find the primary star mass corresponding to each M_V bin.

While calculating the composite mass- M_V relation, the mass we refer to is always the primary star mass, while M_V corresponds to the total M_V of the system. From Duquennoy (1988) we find that there are on an average 0.61 undetected companions per star. We therefore assume that each system is a binary system consisting of a primary star and 0.61 companions. We denote the ratio of the mass of the idealized companion to the primary star mass as q , and although our stellar system is

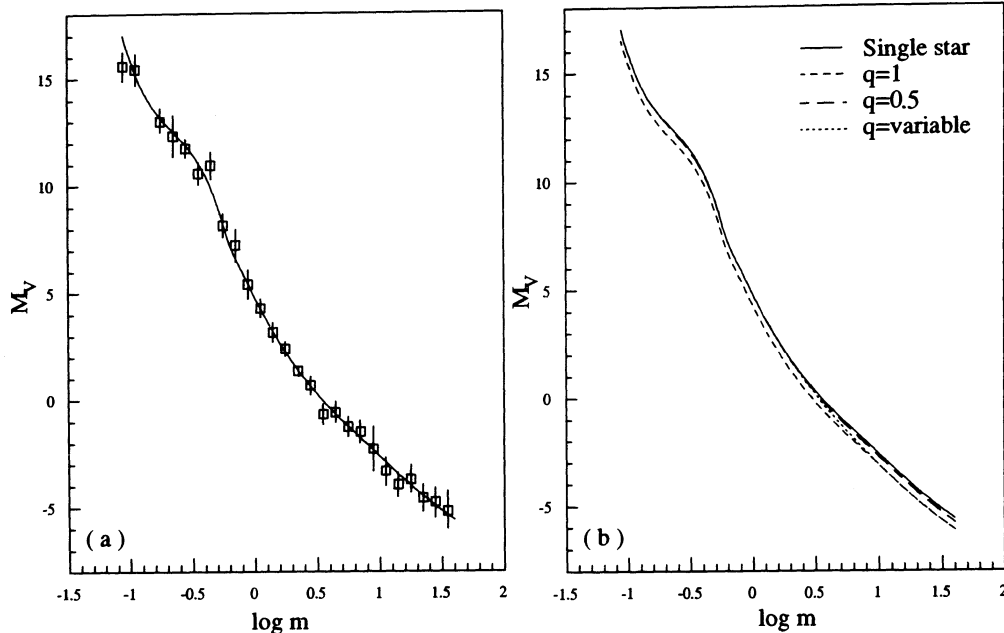


FIG. 1.—(a) m - M_V relation adopted for this work. The squares are the observed data on the m - M_V relation binned at intervals of 0.1 in $\log m$. The solid line through the squares is the relation used in this work. (b) The "composite" m - M_V relations constructed for various values of q assuming 0.61 companions per primary star. The mass here refers to the mass of the primary star only, while the absolute magnitude is that of the whole system.

strictly not a binary system, we use the values of q determined from the existing observations on binary stars.

Most samples of unevolved binaries show a peak at $q = 1$ (Trimble 1974; Lucy & Ricco 1979; Wolff 1978; Abt & Levy 1978; Trimble & Walker 1986). However, Halbwachs (1987) found only a low q peak in a cataloged sample of spectroscopic systems. Trimble & Walker (1986) found a bimodal q distribution for spectroscopic binaries, however, the low q peak is supposed to have a contribution from systems which have gone through a mass transfer phase, and hence does not concern us. Similarly eclipsing binaries also show a low q peak, but since the q distribution of eclipsing binaries reflect mass, energy, and angular momentum transfer rather than the star-formation process (Shu & Lubow 1981), we disregard the sample. Duquennoy & Mayor (1989) working with a sample of G-dwarfs do not find a peak at $q = 1$, but at $q \approx 0.23$. Trimble (1987) looking at common proper pairs and visual binaries could identify a peak at $q = 1$. However, complete subsamples of relatively bright, wide, and close systems show a distribution that is at best flat in q .

Thus the distribution of stars with respect to q is far from clear. We therefore consider three separate cases for the q -distribution. Since there are not enough data, any choice we make will of course be only an approximation of the real situation. As the peak at $q = 1$ is prominent in many samples, in one case we choose $q = 1$ for all systems. However if we take the flat q distribution of Trimble (1987) seriously, we should take an average q of 0.5. This is our second case. Duquennoy & Mayor (1989) find only a low q peak, and so does Halbwachs (1987). The sample of Duquennoy and Mayor was, however, restricted to low-mass stars. As for high-mass stars, Garmany, Conti, & Massey (1980) and Garmany & Conti (1988) find that the mass ratios of unevolved O stars are close to unity. Abt (1983) concurs. Thus for our third case we choose a value of q which increases with the mass of the primary, but is constant at $q = 0.25$ below $1 M_{\odot}$, and $q = 1$ above $10 M_{\odot}$.

To summarize, the three cases we consider are

Case (a):

$$q = 1 ,$$

Case (b):

$$q = 0.5 ,$$

Case (c):

$$\begin{aligned} q &= 0.25 && \text{for } m \leq 1 , \\ &= 0.25 + 0.75 \log m && \text{for } 1 < m < 10 , \\ &= 1.0 && \text{for } m \geq 10 . \end{aligned}$$

Once we know q , we know the mass of the secondary for a given primary mass. The single star $m-M_V$ relation enables us to find the absolute magnitudes, and hence fluxes received from the two components. Thus we can find the total flux from the system, and hence the composite M_V of the system. The composite $m-M_V$ relation will generally show a lower M_V (i.e., higher luminosity) at a given mass compared to the single star $m-M_V$ relation. This is because the mass in the composite $m-M_V$ relation refers to the mass of the primary alone.

In Figure 1b we show the composite $m-M_V$ relation for the various values of q along with the underlying single-star mass-luminosity relation.

We also use the single star $m-M_V$ relation to determine the PDMF without applying any correction for multiplicity. We call this the "uncorrected" PDMF. Thus we shall be dealing with four different cases of the PDMF.

2.2. The Luminosity Function

Our source of the photometric luminosity function (LF) is the compilation in Rana (1990a). The correction for the fraction of stars which have moved off the main sequence has been determined following Scalo (1986).

Since we shall be correcting the LF for the presence of multiple stellar systems, the total number of stars represented by the LF will increase due to the contribution from the secondaries. As the mass of the secondary is not in general equal to the mass of the primary, the contribution to the LF from the secondary component of a system will not be to the same M_V (or mass) bin to which the primary belongs, but to a higher M_V (i.e., a lower mass) bin.

Although when we start off with the photometric luminosity function, we deal with the number of stars per unit range of the absolute V -magnitude, it does not generally remain so once the true luminosity corresponding to the primary star masses at the bin limits is determined. This is because the $m-M_V$ relation is not linear. Hence, to use equation (1), the LF has to be normalized by dividing by the true width of the bin, ΔM_V .

The construction of composite the $m-M_V$ relations for each value of q is justified by Figures 2a and 2b. Both figures show the luminosity function plotted, not against M_V , but against the logarithm of mass corresponding to each value of M_V . The conversion was done using the constructed $m-M_V$ relations. Figure 2a shows the effect of the presence of a companion. The fraction of companions, f is varied, keeping q constant at 1. We can see that the presence of a companion shifts the whole curve to the lower mass end. The nonlinear nature of the $m-M_V$ relation manifests as a nonuniform shift across the entire mass range. The shift in mass of a given point in the luminosity function can be very large, $\approx 30\%$ as the largest. For masses lower than $0.2 M_{\odot}$, we will underestimate the number of stars at a given mass if we do not take the multiple nature of the system into account, while for higher masses we will overestimate the number.

Figure 2b again shows the LF plotted against $\log m$, but this time for different values of q , with the fraction f kept fixed at the adopted value of 0.61. We can see that increasing values of q shift the curve to the lower mass end. For the variable q case we see not merely a shift but a change in the shape of the function too at the high-mass end.

The luminosity function used for this work does not extend below $M_V = -5.5$, i.e., for masses greater than about $30 M_{\odot}$. We therefore have to rely on direct determinations made by various groups of the high-mass end of the PDMF. We have considered the works of Garmany et al. (1982), Bisiacchi et al. (1983), Humphreys & McElroy (1984), and Van Buren (1985). Vanbeveren (1984) was omitted since he has excluded all known binaries from his sample.

If we consider all the determinations together, we find that there is not too small a scatter in the PDMF. This has enabled us to smoothly continue the PDMF we calculate into the high-mass region.

2.3. The Scale Heights

Wielen (1977) showed that the velocity dispersion of stars in the solar neighborhood increases with age. This would imply a

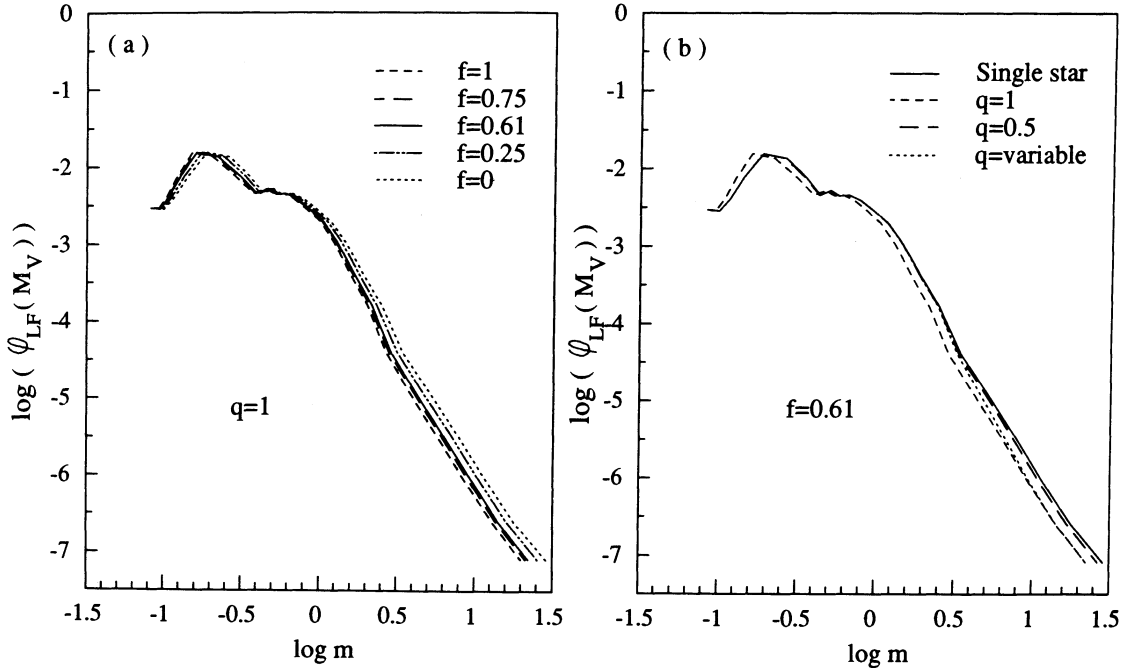


FIG. 2.—Luminosity function has been plotted as a function of mass. The luminosity function is in units of number of stars per parsec³ per unit interval of M_V . (a) The effect of the number of companions per primary star is seen here as a shift in the luminosity function when plotted against mass. The curves have been plotted for a constant value of q . The $f=0$ curve corresponds to the single star case, while $f=1$ represents a true binary system. (b) Effect of the ratio of the companion mass to the primary star mass is also seen as shift with respect to mass. The curves have been drawn for different values of q for a constant value of the number f of companions per primary star. The solid line corresponds to the single star case. A failure to construct the composite m - M_V relation would thus lead to an erroneous mass dependence of the number of stars in the solar neighborhood.

correlation between scale height and age, since the scale height is given by

$$H = \frac{\sigma_z^2}{\pi G \Sigma} \quad (4)$$

for a disk isothermal in the z -direction (Wielen & Fuchs 1983). Here σ_z is the velocity dispersion in the direction normal to the plane of the disk, G is the Newtonian gravitational constant, and Σ is the total surface mass density of the disk. Villumsen (1985) showed that σ_z for such a system at any given time t can be written as

$$\sigma_z \propto \left(1 + \frac{t}{\tau}\right)^n,$$

thus,

$$H(t) = H(0) \left(1 + \frac{t}{\tau}\right)^{2n}. \quad (5)$$

The quantity $H(0)$ is by definition the scale height of stars at birth. We find that the scale height data given in Robin & Cr ez e (1986) can be fitted well with the form given in equation (5) (see Fig. 3a) for $H(0) = 95$ pc, $\tau = 0.5$ Gyr, and $2n = \frac{2}{3}$. The result is encouraging because Wood & Churwell (1989) find that the scale height of OB star-forming regions is about 90 pc. If we hold $H(0)$ fixed at 90 pc, and then find τ and n , the difference in the mean scale heights is only about 0.5% for long-lived stars and $\approx 5\%$ for the short-lived high-mass stars.

Since stars of a given mass m could have been born anytime between the present (a look-back time of $t' = 0$) and a time $t' = t_{\text{ms}}(m)$, the mean scale height for the stars have to be used

and it is given by

$$\langle H \rangle(m) = \int_0^{t_{\text{ms}}(m)} \psi(t_d - t') H(t') dt' / \int_0^{t_{\text{ms}}(m)} \psi(t_d - t') dt', \quad (6)$$

where t' denotes the look-back time.

The averaging however, has the undesirable effect of making the PDMF, which should be an observable quantity, model-dependent. The difference in the average scale heights calculated using the different SFRs listed in the next section is negligible at the high-mass end (less than 1% for stars with $t_{\text{ms}} < 1.6$ Gyr, i.e., $m \gtrsim 2 M_\odot$), increasing rapidly thereafter, becoming about 10% for stars with $t_{\text{ms}} \geq t_d$. The scale heights should ideally be observed quantities, however, since the data are incomplete, like Rana (1991) we adopt the average scale heights calculated for $\psi(t) = \text{constant}$. The difference between the results for the various SFRs is added as an error to the result. The mean scale height as a function of mass is shown in Figure 3b.

All components of a multiple system will be at the same height above the Galactic disk. However, since the primary star of a system is the star with the higher mass, it will not live long enough to reach the terminal scale height of the secondary. Thus when we calculate the contribution of the secondary components in the LF, the scale height we have to multiply it with to get the number of secondaries per unit area is the mean scale height of the primary component. Mathematically, we may therefore write the corrected PDMF as

$$\begin{aligned} \phi_{\text{ms}}(\log m) &= 2 \left[\frac{\phi_{\text{LF}}(M_V)}{\Delta M_V} \langle H \rangle(m) + S(m') \right] \left| \frac{dM_V}{d \log m} \right| \\ &= \phi_{\text{ms}}^{(1)}(\log m) + \phi_{\text{ms}}^{(2)}(\log m'), \end{aligned} \quad (7)$$

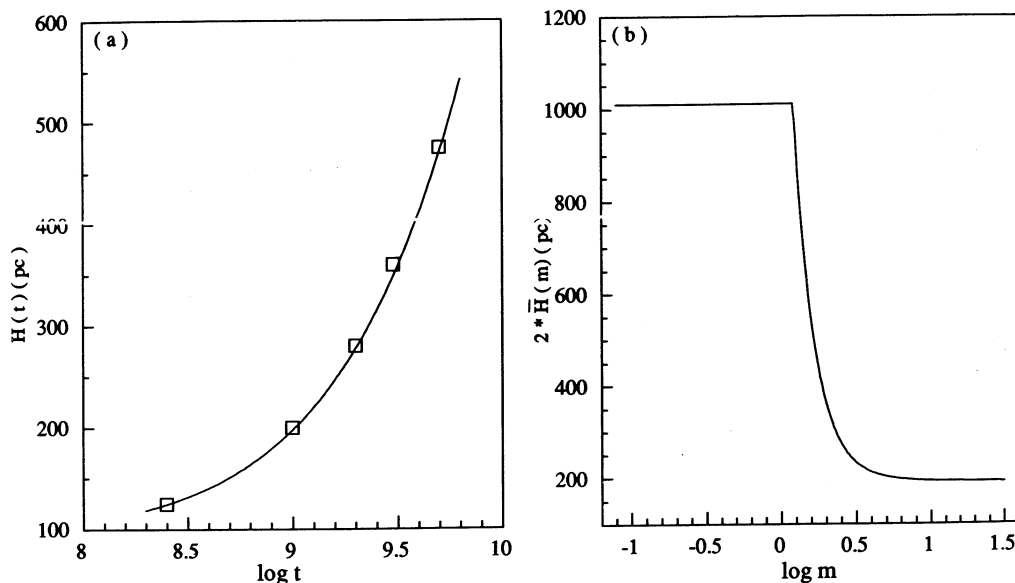


FIG. 3.—(a) Scale height $H(t)$ in units of pc is plotted as a function of time. The squares are data from Robin & Cr ez e (1986). The solid line is the relation adopted for this work. (b) Twice the mean scale height ($2\langle H \rangle$) is plotted as a function of stellar mass. The curve becomes flat for stellar masses below the mass for which the main-sequence lifetime is equal to the age of the disk.

where $\langle H \rangle(m)$ is the mean scale height of a single star of mass m , $S(m)$ is the contribution of secondaries of multiple systems with primary mass m' , such that $m = q(m')m'$, and therefore,

$$S(m) = 0.61 \frac{\phi_{\text{LF}}(M'_V)}{\Delta M'_V} \langle H \rangle(m'). \quad (8)$$

2.4. The Star Formation Rate

The SFR is a very model dependent quantity since there are no observations which can accurately determine the history of star formation in the solar neighborhood. Miller & Scalo (1979) from a study of the IMF, and Twarog (1980) and Carlberg et al. (1985) from studies of metallicity distribution in F-stars conclude that the SFR has basically remained constant over the age of the Galactic disk, with the ratio of the past average to the present SFR in the range 2.5 to 0.5. Thus one of the SFRs we consider is one which remains constant throughout the age of the disk.

Following Tosi & D iaz (1985) and Tosi (1988) we try an SFR of the form $\psi \propto \exp(-t/\tau)$, with $\tau = 15$ Gyr which is said to give good fits to functions like the radial variation of the SFR and metallicity in the Galaxy. Since Miller & Scalo (1979) say that the past SFR might actually have been smaller than the present SFR, we also try a slowly increasing SFR with the same form as the above, that is $\psi \propto \exp(-t/\tau)$, but with $\tau = -15$ Gyr.

A closed-box model of the solar neighborhood, with finite initial metallicity and a finite mass of stars at the beginning of the disk, with the metallicity distribution of G-dwarfs and the age-metallicity relation as the input parameters, yields an SFR which may be written as $\psi \propto \Sigma_g$, where Σ_g is the surface mass density of gas (Rana 1991). This SFR is a rapidly decreasing function of time, and the IMF derived using this SFR is almost identical to the one derived using an SFR of the form $\psi \propto \exp(-t/\tau)$, with $\tau = 5$ Gyr. Since the exponential dependence of the SFR is easier to handle than the form with explicit gas density and metallicity dependence, as the fourth form of SFR we use $\psi \propto \exp(-t/\tau)$, with $\tau = 5$ Gyr. Thus we basically have

four SFRs of the same form which can be summarized as

$$\psi_s \propto \exp(-t/\tau),$$

with

- (1) $\tau = \infty$,
- (2) $\tau = 15$ Gyr,
- (3) $\tau = -15$ Gyr,
- (4) $\tau = 5$ Gyr.

2.5. The Main-Sequence Lifetime of Stars

Data on the main-sequence lifetime of stars have been taken from Maeder & Meynet (1989) and Maeder (1990), and can be fitted with a polynomial of degree five of the form

$$\begin{aligned} \log t_9 = & (1.043 \pm 0.002) - (4.329 \pm 0.012) \log m \\ & + (0.787 \pm 0.009)(\log m)^2 + (0.973 \pm 0.005)(\log m)^3 \\ & - (0.612 \pm 0.003)(\log m)^4 + (0.110 \pm 0.001)(\log m)^5. \end{aligned} \quad (9)$$

where

$$t_9 = t_{\text{ms}}/10^9 \text{ yr}.$$

The lifetimes used here are in general larger for a given mass than those used in Rana (1990a). This would mean that for stars of mass larger than the turnoff mass m_t [$=m(t_d)$], the derived IMF will be smaller.

Since we are dealing with multiple systems, we cannot calculate the IMF directly using equation (2) with lifetimes given by equation (9). Once the primary finishes its main-sequence phase, we assume that the secondary with the lower mass too has ended its main-sequence evolution due to mass received from the primary. Thus for stars of a given mass we have to apply equation (2) separately for stars which are the primary stars of multiple systems and for those which are the secondary components of systems with more massive primaries. There-

fore, we may write

$$\xi(\log m) = E(m)\phi_{\text{ms}}^{(1)}(\log m) + E(m')\phi_{\text{ms}}^{(2)}(\log m'), \quad (10)$$

where $\phi_{\text{ms}}^{(1)}(\log m)$ and $\phi_{\text{ms}}^{(2)}(\log m')$ are defined in equation (7) and m' is the mass of the primary star of a multiple system whose secondary has a mass m , therefore $m = q(m')m'$.

2.6. The Age of the Galactic Disk

The upper limit to the age of the disk is generally assumed to be the lower limit to the age of globular clusters of the Galaxy. The age of the youngest known globular cluster, 47 Tuc, is supposed to be around 13.5 ± 2 Gyr (Buonanno, Corsi, & Fusi Pecci 1989). Using the Th/Nd ratio, Malaney, Mathew, & Dearborn (1989) finds that t_d should be about 12 ± 1 Gyr, and from the Th/U ratio, Meyer & Schramm (1986) find the age of the disk to be 11 Gyr. For nearby disk stars, Grennon (1989) finds the maximum age to be 11 to 12 Gyr. We therefore adopt $t_d = 12$ Gyr for this work.

3. RESULTS AND DISCUSSION

3.1. The PDMF

3.1.1. The Derived PDMF

The calculated PDMFs are shown in Figure 4. For reasons of clarity we have not plotted the points corresponding to the

PDMFs for the different values of q , but have drawn straight lines through the points. Nor have we shown the error bars.

The error in the PDMF is calculated as follows. We obtain an error of about 5% due to the uncertainties in the parameters of the scale height. A further 10% error due to the scale height is added at the low-mass end (for masses less than $1.3 M_{\odot}$), in order to keep the PDMF model independent despite the scale height parametrization used. We estimate a further 20% error over the entire mass range due to uncertainties in the mass-luminosity relation and the lifetimes of stars.

As can be seen very clearly from Figure 4, the main effect of multiplicity of stars shows up at the low-mass end. The effect of having different values of q also manifests at the low-mass end. The high-mass end is almost identical for all the PDMFs whether or not they have been corrected for multiplicity.

The uncorrected PDMF, and the PDMF for $q = 1$ show two peaks. The dip in between appears at $m = 0.44$ for the uncorrected case, and at $m = 0.2$ in the $q = 1$ case. One must, however, be a bit cautious about the dip. It is only about 30% lower than the peak, and the uncertainties in the PDMF at this mass range is about 23%.

The PDMF for the $q = 0.5$ case, the dip becomes shallower, and the peak at the lower mass end is broader. In fact within the error bars it is quite consistent with a flat PDMF at the low mass end. The only anomaly is the point (corresponding to the

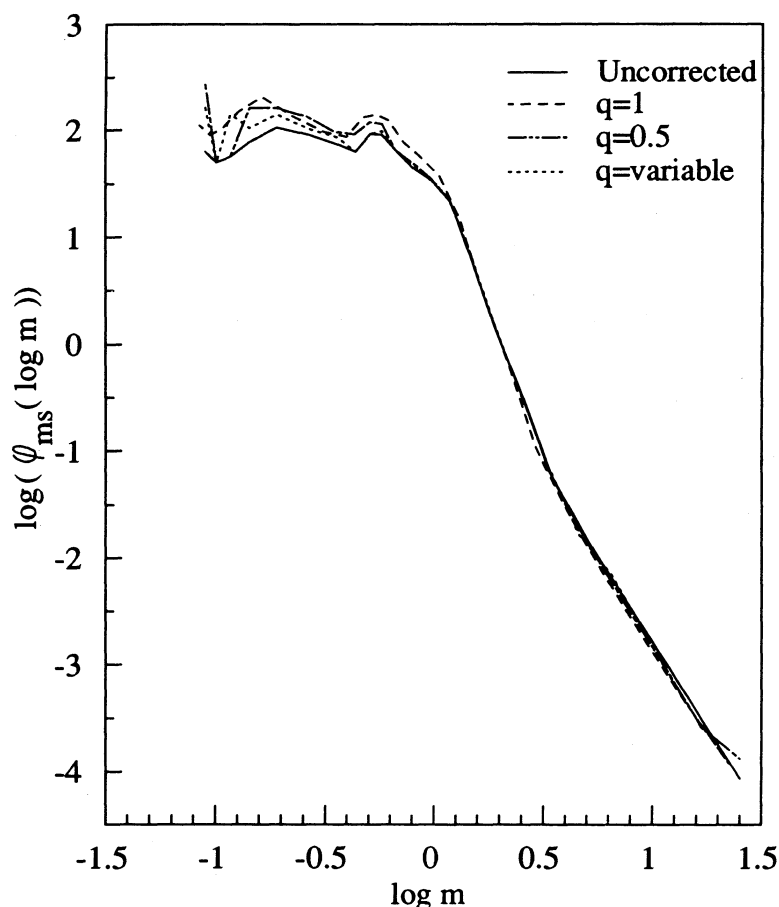


FIG. 4.—Derived PDMFs for various values of the ratio q of the companion mass to the primary star mass with each primary star assumed to have 0.61 companions. The PDMF calculated without corrections for multiplicity is shown as a solid curve. The error bars are not plotted for the sake of clarity. The PDMF is in units of number of stars per parsec² per unit logarithmic interval of mass.

lowest mass) which rises sharply. This rise is mainly due to the steep $m-M_V$ relation at that mass, but is compounded by a slight rise in the LF at that mass. Even more consistent with a flat PDMF at the low mass end is the PDMF calculated for the variable q case.

Since there is no criterion to choose among the three different PDMFs calculated using the three different values of q , for further work we take the average of the three sets.

3.1.2. The Average PDMF

The second column of Table 1 lists the PDMF we use for further calculations. Henceforth we shall call it the "corrected" PDMF in contrast to the "uncorrected" PDMF which was calculated without any correction for multiplicity. Figure 5 shows the corrected and uncorrected PDMFs. We can see that the average corrected PDMF and the uncorrected one have practically the same shape. However, the curve for the corrected PDMF is placed higher than that for the uncorrected one. This is expected since the number of stars increases once multiplicity is taken into account.

The shape of the PDMF shown in Figure 5 is very different from those in Rana (1987) and Rana (1990a). The PDMF in Scalo (1986) too is very different. The PDMF looks bimodal. However, since the dip following the first peak is not very deep (it is only 30% lower than the peak), and also since the point corresponding to the lowest mass rises sharply, we cannot rule out the possibility of a flat PDMF in this mass range. D'Antona & Mazzitelli (1986) find that the mass function at the low-mass end rises with a power-law index of -2.04 ± 0.40

for the mass range $0.3 > m > 1.0$, however we do not find such a smooth function here.

On integrating the corrected PDMF between the mass range $0.08 \leq m \leq 100$, we find that the PDMF shows the presence of $113.8^{+36.0}_{-27.3}$ stars pc^{-2} in the solar neighborhood. In terms of mass, it accounts for $39.6^{+12.4}_{-9.5} M_{\odot} \text{pc}^{-2}$ in the disk. On integrating the uncorrected PDMF over the same mass range we obtain only $31.3^{+9.2}_{-7.1} M_{\odot} \text{pc}^{-2}$. The mass calculated from the corrected PDMF is larger than the mass calculated from the PDMFs of Scalo (1986) or Rana (1987, 1990a).

3.2. The IMF

3.2.1. The General Form of the IMF

Figure 6 shows the initial mass functions derived using the corrected PDMF and the four different forms of the SFR mentioned in § 2.4. The IMFs are also listed in Table 1. All the IMFs are almost parallel at the high-mass end. The IMF for the rapidly decreasing SFR with a time constant of 5 Gyr shows a hump between $m = 1.1$ and 2.3. This feature is an artifact of the rapid decrease of the SFR as has been discussed quite extensively in Scalo (1986).

All the IMFs in Figure 6 show a rapid fall till about $m = 6$, where they become less steep. However, the steep descent continues thereafter.

For masses greater than $0.56 M_{\odot}$, the IMF can be fitted by a power law. The fit is the best for the IMF calculated for the SFR with an exponential decrease with a time constant of $\tau = 15$ Gyr (slope = 1.58 ± 0.07). The power-law fit is not very

TABLE 1
THE CORRECTED PDMF AND THE IMFs

log m	$\sigma_{\log m}$	log $\phi_{\text{ms}}(\log m)$	σ_{PDMF}	log [$\xi(\log m)$]			
				$\tau = \infty$	$\tau = 15$ (Gyr)	$\tau = -15$ (Gyr)	$\tau = 5$ (Gyr)
-1.06.....	0.01	2.22	0.16	2.22	2.22	2.22	2.22
-1.01.....	0.01	1.78	0.12	1.78	1.78	1.78	1.78
-0.94.....	0.02	1.97	0.16	1.97	1.97	1.97	1.97
-0.86.....	0.02	2.13	0.11	2.13	2.13	2.13	2.13
-0.75.....	0.03	2.22	0.11	2.22	2.22	2.22	2.22
-0.60.....	0.03	2.09	0.11	2.09	2.09	2.09	2.09
-0.47.....	0.03	1.97	0.11	1.97	1.97	1.97	1.97
-0.38.....	0.02	1.90	0.11	1.89	1.89	1.89	1.89
-0.31.....	0.01	2.05	0.11	2.05	2.05	2.05	2.05
-0.25.....	0.01	2.06	0.11	2.08	2.08	2.07	2.10
-0.19.....	0.02	1.90	0.13	1.90	1.90	1.90	1.90
-0.12.....	0.02	1.75	0.11	1.78	1.80	1.77	1.85
-0.03.....	0.02	1.61	0.11	1.63	1.64	1.62	1.68
0.05.....	0.02	1.42	0.11	1.45	1.46	1.44	1.51
0.15.....	0.02	0.94	0.16	1.24	1.34	1.17	1.57
0.25.....	0.03	0.29	0.14	1.03	1.18	0.90	1.54
0.37.....	0.03	-0.34	0.13	0.80	0.97	0.65	1.38
0.50.....	0.03	-1.10	0.10	0.51	0.69	0.35	1.12
0.66.....	0.03	-1.73	0.10	0.27	0.45	0.11	0.88
0.82.....	0.03	-2.25	0.10	0.14	0.32	-0.03	0.77
1.00.....	0.03	-2.83	0.10	-0.11	0.08	-0.27	0.53
1.18.....	0.03	-3.44	0.11	-0.45	-0.27	-0.61	0.18
1.37.....	0.02	-3.91	0.10	-0.69	-0.50	-0.85	-0.04
1.41.....	0.01	-4.02	0.20	-0.76	-0.57	-0.92	-0.11
1.60.....	0.00	-4.55	0.20	-1.13	-0.94	-1.29	-0.48
1.80.....	0.00	-5.05	0.20	-1.50	-1.32	-1.66	-0.85
1.95.....	0.00	-5.38	0.20	-1.77	-1.58	-1.93	-1.12
2.00.....	0.00	-5.50	0.30	-1.87	-1.90	-2.03	-1.22

NOTE.— $\phi_{\text{ms}}(\log m)$ and $\xi(\log m)$ are in units of number of stars per pc^2 per unit interval of the logarithm of mass.

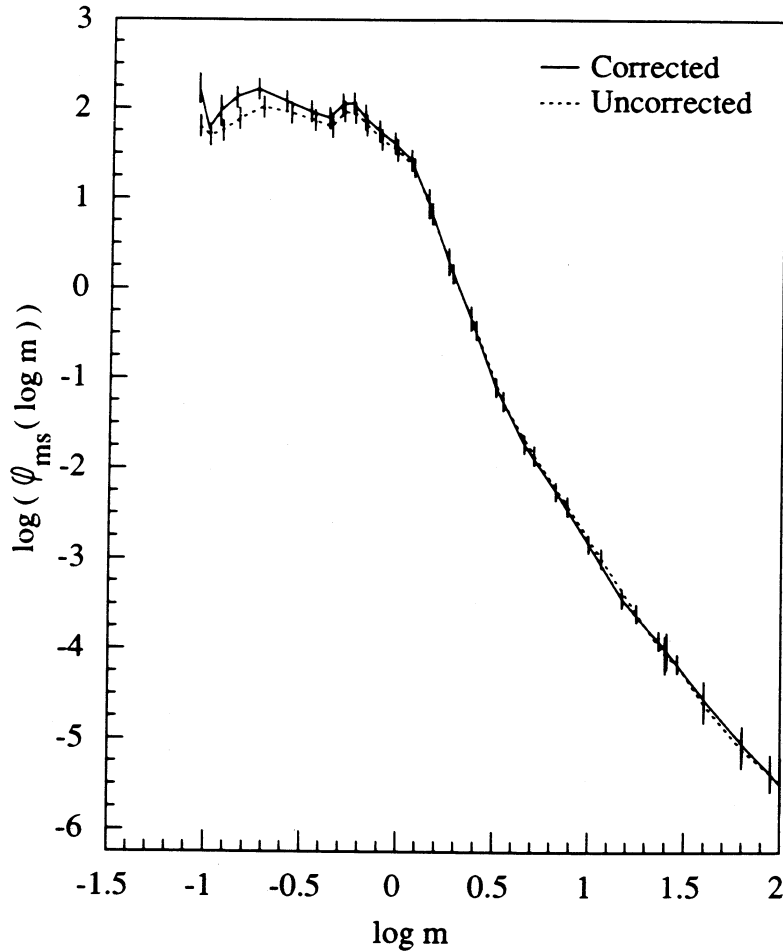


FIG. 5.—Average corrected PDMF and the uncorrected PDMF are shown for comparison. The PDMF is in units of number of stars per parsec² per unit logarithmic interval of mass. The corrected PDMF on integration gives a surface mass density of $39.5 M_{\odot} \text{ pc}^{-2}$ for the Galactic disk, while the uncorrected PDMF gives only $31.3 M_{\odot} \text{ pc}^{-2}$.

good for the IMF calculated using the SFR which is an increasing function of time ($\tau = -15 \text{ Gyr}$), but it still gives a reduced χ^2 of less than one ($\chi^2 = 0.98$). The average slope ($-x$) is a strong function of τ , with an approximate form

$$\langle x \rangle \approx (1.69 \pm 0.10) - (1.5 \text{ Gyr}/\tau). \quad (11)$$

Above $m = 1.4$, the IMFs become almost parallel. The power-law fits are even better with almost identical exponents. If we look at the IMFs at even greater masses, especially after the flattening at $6 M_{\odot}$, we find that all the IMFs can be fitted with a single power law having an exponent of -1.67 ± 0.04 for $m \geq 6.5$. Table 2 tabulates the parameters of the power-law fit for the different mass ranges.

The IMFs cannot be fitted very satisfactorily to any simple polynomial form over the entire mass range. If the point at the lowest mass point is ignored, $\log \zeta(\log m)$ can be fitted to a polynomial of degree four in $\log m$. The parameters of the fit, and the resultant χ^2 -values are listed in Table 2. The quartic fit reproduces the flattening at $m = 6$. It cannot however, reproduce the two peaks at the low-mass end. It may be mentioned that our attempt to obtain a lognormal fit for $\zeta(\log m)$ has been quite unsatisfactory. Only the IMF for $\tau = 5 \text{ Gyr}$ gives a reduced χ^2 of less than 1.

All the IMFs that have been calculated show two peaks at the low-mass end, one at $0.18 M_{\odot}$ and the other at $0.56 M_{\odot}$. Also present in the $\log m$ - $\log \zeta(\log m)$ plot is a change in slope around 5 - $6 M_{\odot}$. This change in slope appears as a broad plateau in a $\log m$ - $\log [m\zeta(\log m)]$ plot. A fourth feature at $30 M_{\odot}$ is probably a real feature, but its properties and shape would depend on the extrapolation of the PDMF at higher masses. The presence of these features means that we are probably justified in calling the IMFs multimodal.

An IMF which deviates from a power law at the high-mass end is not unexpected from theory. IMFs computed while taking into account the simultaneous presence of several instability criteria for fragmentation—like magnetic, rotational, turbulent, etc.—can give rise to a number of humps in the high-mass end of the IMF (Ferrini, Palla, & Penco 1990).

3.2.2. A Few Derived Quantities

In Table 3 we have tabulated various quantities that can be derived from the IMF, like the total number of stars formed to date per unit area of the solar neighborhood (N_{IMF}), the total surface mass density of stars formed (Σ_{IMF}), the surface mass density of gas returned to the interstellar medium by stars at the end of their lives (Σ_{ret}), the surface mass density of remnants

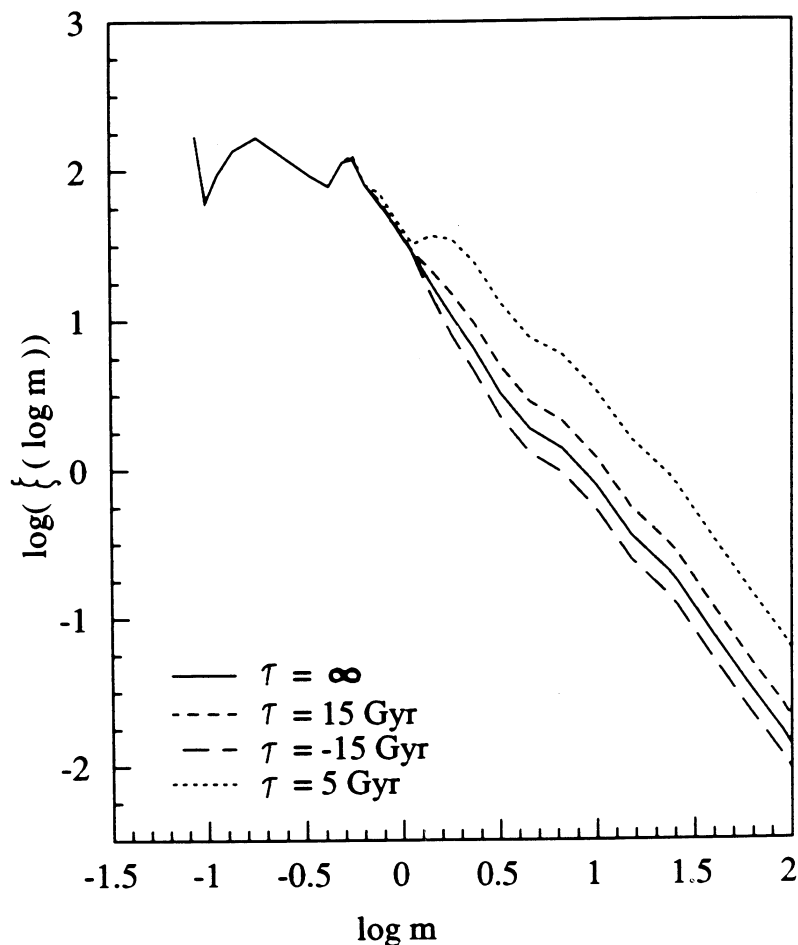


FIG. 6.—Initial mass function of stars in the solar neighborhood calculated for different star-formation rates. The star-formation rates per unit area of the local disk are assumed to have the form $\psi_s \propto \exp(-t/\tau)$, but with different values of the exponential time constant τ . The IMF is in units of number of stars per parsec² per unit logarithmic interval of mass.

(Σ_{rem}), the surface mass density of evolved stars (Σ_{ev}), the calculated total surface mass density (Σ_T), the average SFR ($\langle\psi_s\rangle$), and the present SFR (ψ_s)₁ (see Rana 1987 for the formulae).

In order to find the total number and the total mass densities of stars, we have integrated the IMF in the mass range $0.08 \leq m \leq 100$. While finding the remnant mass and the returned mass, the lower limit of integration here has been taken as $1.3 M_\odot$ because stars with a lower mass have total lifetimes greater than the age of the Galactic disk, and hence do not leave a remnant behind.

We have considered a very simple prescription for the mass of the remnant left behind by a star of any given mass in order to calculate the total remnant mass and the mass of gas returned to the ISM. Since stars of mass less than $1.3 M_\odot$ have not died in the lifetime of the Galactic disk, the question of a remnant mass for them is quite irrelevant. For heavier stars of mass up to $3.5 M_\odot$, we assume a remnant white dwarf mass of $0.6 M_\odot$. Beyond that the remnant mass is assumed to increase monotonically to $1.4 M_\odot$ for a star of mass $6.5 M_\odot$. The single-star progenitors of Type I supernovae are supposed to lie in the mass range $6.5 M_\odot$ to $8 M_\odot$. Since a Type I supernova is supposed to disintegrate the star totally, the remnant mass is zero for this range of masses. Beyond that we assume a constant neutron star mass of $1.4 M_\odot$ as the remnant mass.

The total accountable baryonic surface mass density in Table 3 is the sum of the mass densities of stars present as main-sequence stars, of evolved stars, of remnants and the leftover gas. Assuming that the interstellar gas in solar neighborhood consists of 70% by mass of hydrogen, the amount of leftover gas in the solar neighborhood is about $6.6 M_\odot \text{ pc}^{-2}$ (from Bronfman et al. 1988 and Bhat et al. 1985 for molecular hydrogen, and Burton & Gordon 1978 and Li, Riley, & Wolfendale 1982 for the atomic hydrogen mass).

We have also tabulated the “returned fraction” $R(= \Sigma_{\text{ret}}/\Sigma_{\text{IMF}})$ i.e., the ratio of the mass returned to the ISM to the total mass that has gone into star formation. The fraction of remnants $D(= \Sigma_{\text{rem}}/\Sigma_{\text{IMF}})$, and the fraction of evolved stars $E(= \Sigma_{\text{ev}}/\Sigma_{\text{IMF}})$ are also shown.

The trends in the various derived quantities are very clear. The total number and the total mass of stars formed per square parsec of the local disk since the birth of the disk increase with an increase in $(1/\tau)$, where τ is the time scale of star formation. The same trend is seen for the returned and remnant masses and the mass of evolved stars. Hence the fractions R , D , and E show the same trend.

The current star-formation rate is observationally estimated to be around $3.5 M_\odot \text{ pc}^{-2} \text{ Gyr}^{-1}$ to $5 M_\odot \text{ pc}^{-2} \text{ Gyr}^{-1}$ in the solar neighborhood (Talbot 1980; Smith, Biermann, & Mezger

TABLE 2
PARAMETERS FOR ANALYTIC FITS TO THE IMFs

PARAMETER	IMFs FOR SFRs WITH			
	$\tau = \infty$	$\tau = 15$ (Gyr)	$\tau = -15$ (Gyr)	$\tau = 5$ (Gyr)
Power-Law Fit: $\xi(\log m) = am^{-x}$				
(1) $0.56 \leq m \leq 100$:				
a	$33.9^{+6.9}_{-5.7}$	$38.9^{+5.8}_{-5.0}$	$30.2^{+9.6}_{-7.3}$	$55.0^{+14.2}_{-11.3}$
x	1.69 ± 0.10	1.58 ± 0.07	1.79 ± 0.14	1.32 ± 0.12
χ^2	0.52	0.25	0.98	0.69
(2) $1.4 \leq m \leq 100$:				
a	$24.0^{+3.5}_{-3.1}$	$34.7^{+5.1}_{-3.0}$	$17.8^{+3.1}_{-2.6}$	$79.2^{+13.3}_{-11.4}$
x	1.56 ± 0.06	1.54 ± 0.05	1.59 ± 0.07	1.45 ± 0.07
χ^2	0.25	0.22	0.32	0.29
(3) $6.65 \leq m \leq 100$:				
a	$34.7^{+2.5}_{-1.6}$	$52.5^{+3.8}_{-3.5}$	$23.4^{+1.7}_{-1.6}$	$143.3^{+10.2}_{-9.6}$
x	1.67 ± 0.03	1.67 ± 0.03	1.67 ± 0.03	1.65 ± 0.03
χ^2	0.08	0.08	0.07	0.08
Quartic Fit: $\log \xi(\log m) = a_0 + a_1(\log m) + a_2(\log m)^2 + a_3(\log m)^3 + a_4(\log m)^4$				
a_0	1.52 ± 0.08	1.57 ± 0.08	1.47 ± 0.10	1.72 ± 0.08
a_1	-1.71 ± 0.10	-1.51 ± 0.10	-1.89 ± 0.12	-1.04 ± 0.10
a_2	-0.46 ± 0.08	-0.44 ± 0.08	-0.47 ± 0.10	-0.40 ± 0.08
a_3	0.71 ± 0.06	0.59 ± 0.05	0.81 ± 0.06	0.33 ± 0.05
a_4	-0.24 ± 0.03	-0.20 ± 0.03	-0.27 ± 0.04	-0.12 ± 0.03
χ^2	0.49	0.40	0.59	0.42

1978). Our estimates of the current SFR from the derived IMFs lie well within this range except for the SFR with $\tau = 5$ Gyr. The current SFR for that model is $1.94^{+0.64}_{-0.48} M_{\odot} \text{pc}^{-2} \text{Gyr}^{-1}$, which is slightly lower than the observational estimates.

The star-formation rate and the IMF can be used to calculate the current and the past average rate of formation of neutron stars (Rana 1991). Our results are tabulated in Table 4.

There is no clear consensus on the rate of formation of neutron stars. There have been a number of attempts to determine this rate (Van den Bergh, McClure, & Evans 1987; Caswell & Lerche 1979; Blaauw 1985; Narayan 1986), and varies from about $0.010 \text{pc}^{-2} \text{Gyr}^{-1}$ to $0.031^{+0.156}_{-0.007} \text{pc}^{-2} \text{Gyr}^{-1}$. On comparing the entries in Table 4 with these results, we find that the neutron star birth rates predicted by the IMF agree with the observational estimates for all SFRs except that with $\tau = 5$ Gyr. This SFR predicts higher rates than is observed.

As in the case of neutron stars, the rate of formation of white dwarfs can also be predicted from the IMF (Rana 1991). The white dwarf formation rate per unit volume C_{WD}^V , is plotted as a function of look-back time in Figure 7. Also shown on the figure are the rates of white dwarf formation calculated from

the white dwarf luminosity function and white dwarf cooling curves as used by Rana (1989) and Rana (1990b). The rate of white dwarf formation seems to agree reasonably well with the predictions of the IMFs calculated with SFRs with $\tau = -15, 0$, and 15 Gyr. But the $\tau = 5$ Gyr case predicts a bit too high of a rate and lies above the upper error limits of all the points in Figure 7.

3.2.3. The Problem of Disk Dark Matter in the Solar Neighborhood

From dynamical considerations, the total surface mass density in the solar neighborhood was estimated to be $54 \pm 8 M_{\odot} \text{pc}^{-2}$ by Gould (1990) and $48 \pm 8 M_{\odot} \text{pc}^{-2}$ by Kuijken & Gilmore (1991). If we look at the column for total mass density, we find that we require no nonbaryonic dark matter to account for the mass density estimated by dynamical means. It must be noted that we have only considered stellar masses greater than $0.08 M_{\odot}$ to calculate the total mass in stars. We have not given any mass estimates for stars of a lower mass, i.e., the brown dwarfs or planets. There is considerable debate about the shape of the IMF at very low masses, but whatever the mass dependence, the very presence of brown dwarfs will increase our estimate of the observed total surface mass density of the

TABLE 3
QUANTITIES DERIVED FROM THE IMFs

IMFs for SFRs with	N_{IMF} (stars pc^{-2})	Σ_{IMF} ($M_{\odot} \text{pc}^{-2}$)	Σ_{ret} ($M_{\odot} \text{pc}^{-2}$)	Σ_{rem} ($M_{\odot} \text{pc}^{-2}$)	Σ_{ev} ($M_{\odot} \text{pc}^{-2}$)	Σ_{tot} ($M_{\odot} \text{pc}^{-2}$)	$(\dot{M}_{\odot})_1$ ($M_{\odot} \text{pc}^{-2} \text{Gyr}^{-1}$)	$\dot{\psi}_{\frac{1}{2}}$ ($M_{\odot} \text{pc}^{-2} \text{Gyr}^{-1}$)	R	D	E
$\tau = 0$	$118.5^{+37.7}_{-28.5}$	$53.7^{+17.2}_{-12.9}$	$10.9^{+3.8}_{-2.7}$	$2.4^{+0.8}_{-0.6}$	$0.9^{+0.2}_{-0.2}$	$49.4^{+12.4}_{-9.4}$	$4.5^{+1.4}_{-1.1}$	$4.5^{+1.4}_{-1.1}$	0.204	0.044	0.016
$\tau = 15$ (Gyr)	$120.9^{+38.5}_{-29.1}$	$61.1^{+19.7}_{-14.8}$	$16.6^{+6.4}_{-5.1}$	$3.6^{+1.2}_{-0.9}$	$1.4^{+0.6}_{-0.4}$	$51.1^{+12.5}_{-9.5}$	$3.3^{+1.1}_{-0.8}$	$5.1^{+1.6}_{-1.2}$	0.272	0.058	0.022
$\tau = -15$ (Gyr)	$117.1^{+15.7}_{-28.1}$	$49.3^{+15.7}_{-11.8}$	$7.47^{+2.6}_{-1.7}$	$1.6^{+0.6}_{-0.4}$	$0.6^{+0.2}_{-0.3}$	$48.4^{+12.4}_{-9.4}$	$6.0^{+1.9}_{-3.8}$	$4.1^{+1.3}_{-1.0}$	0.152	0.033	0.013
$\tau = 5$ (Gyr)	$131.5^{+42.0}_{-31.7}$	$97.1^{+31.8}_{-23.7}$	$45.3^{+15.4}_{-11.3}$	$9.2^{+3.2}_{-2.1}$	$3.1^{+0.9}_{-0.9}$	$58.4^{+12.8}_{-9.7}$	$1.9^{+0.6}_{-0.5}$	$8.1^{+6.6}_{-2.0}$	0.467	0.094	0.032

TABLE 4
THE PREDICTED NEUTRON STAR FORMATION RATES

MASS RANGE (M_{\odot})	NS FORMATION RATES (STARS $\text{pc}^{-2} \text{Gyr}^{-1}$) FOR IMFs WITH							
	$\tau = \infty$		$\tau = 15$		$\tau = -15$		$\tau = 5$	
	Current	Average	Current	Average	Current	Average	Current	Average
8-40	0.020	0.020	0.018	0.035	0.018	0.016	0.019	0.099
8-60	0.021	0.021	0.019	0.036	0.019	0.016	0.020	0.103
9-40	0.016	0.016	0.015	0.028	0.015	0.013	0.016	0.081
9-60	0.017	0.017	0.016	0.030	0.016	0.013	0.017	0.085
10-40	0.013	0.013	0.013	0.023	0.013	0.010	0.014	0.066
10-60	0.013	0.013	0.012	0.025	0.013	0.011	0.014	0.071

NOTE.— τ is in units of Gyr.

baryonic matter in the solar neighborhood. Thus the amount of nonbaryonic dark matter, if any, must be very small.

4. CONCLUSIONS

The aim of the present work was to derive the present-day mass function and the initial mass function of stars in the solar neighborhood after correcting the luminosity function for the effects of unresolved multiple systems. In the process the latest available stellar lifetime data calculated after taking into account effects of mass loss and convective overshoot have been used. A consistent semi-analytical form for the scale-height evolution of stars has been used in order to calculate the

PDMF from the luminosity function, and to calculate the IMF we have an SFR of the form which gives a good fit to data on chemical evolution. We draw the following conclusions from this work:

1. The correction of the PDMF for the multiplicity of stars is important in the sense that it increases the total number of stars represented by the PDMF. The averaged correction for different ratios of the secondary to the primary star mass does not change the shape of the PDMF, but shifts it to the lower mass side.
2. The corrected PDMF on integrating over the mass range $0.08 \leq m \leq 100$ gives a surface mass density of $39.6_{-9.4}^{+12.4} M_{\odot}$.

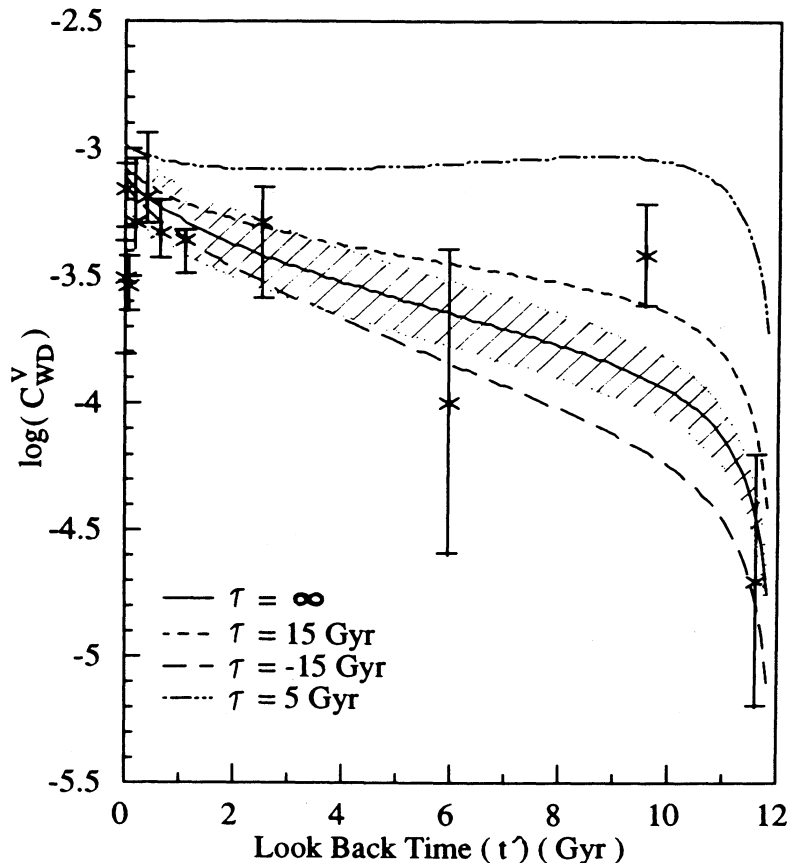


FIG. 7.—Rate of formation of white dwarfs per unit volume of the local disk is shown as a function of look-back time. The hatched area is the error limit for the constant SFR case. The other rates have similar errors. The points plotted are white dwarf formation rates calculated from the white dwarf luminosity function and their cooling curves taken from Rana (1990b). C_{WD}^V is in units of number of white dwarfs $\text{pc}^{-3} \text{Gyr}^{-1}$.

pc^{-2} in the disk main-sequence stars in the solar neighborhood. The uncorrected PDMF gives only $31.3^{+9.2}_{-7.1} M_{\odot} \text{pc}^{-2}$. Although this number is much greater than $22 M_{\odot} \text{pc}^{-2}$ given by Scalo (1986), it is somewhat less than the estimate of Rana (1987) of $32\text{--}35 M_{\odot} \text{pc}^{-2}$. This difference is due to the differences in the LF, the mass-luminosity relation and the scale heights used.

3. The total surface mass density of the Galactic disk in the solar neighborhood predicted by the IMFs is such that very little or no nonbaryonic dark matter is required to account for the total dynamical mass of the Galactic disk in the solar neighborhood.

4. The high-mass end of the IMF can be represented by a power law in stellar mass for the assumed star-formation rates varying exponentially with time. The exponent for the IMF over the mass range $0.56 < m < 100$ becomes more negative with a decrease in $(1/\tau)$, where τ is the exponential time constant of star formation. For masses greater than $6.5 M_{\odot}$, the exponent of the power law becomes practically independent of the law of SFR with a value of about -1.67 ± 0.02 compared to -1.35 due to Salpeter (1955). For IMFs calculated using a constant or slowly varying star-formation rates, the IMF can be represented as a power-law with an exponent of -1.56 ± 0.05 over the entire mass range greater than $1.4 M_{\odot}$. No satisfactory fit could be obtained for the lognormal distribution.

5. The trend in the low mass end of the IMF is not very clear. It looks bimodal, but the difference between the peak and the dip is barely 30% with errors in the range of 20%–25%. The

low mass end is therefore not inconsistent with a flat mass spectrum or even with a gradual turnover.

6. The possibility of a multimodal IMF as indicated by Rana (1987) cannot be ruled out.

7. The ratio of the mass of gas returned to the ISM by the stars to the total mass of gas that has ever gone into forming stars—the returned fraction R —is found to be rapidly increasing function of $(1/\tau)$. The fraction of remnants and evolved stars also increase as $(1/\tau)$ increases, but the increase is not so dramatic.

8. The neutron star-formation rates predicted by the IMFs match the observed rates very well. This is, however, not true for the IMF calculated with an SFR with τ as small as 5 Gyr, the rates predicted by this IMF being much higher than the observed rates.

9. The predicted rate of formation of white dwarfs matches well with the rate calculated from the white dwarf luminosity function and cooling curves for all the IMFs except for that with $\tau = 5$ Gyr.

10. The neutron star and white dwarf formation rates can be used to constrain τ , the exponential time constant of star formation. If we are to predict a reasonable rate of neutron star and white dwarf formation compatible with observations, τ shall have to be restricted to the range $-0.1 \leq (1/\tau) \leq +0.1 \text{ Gyr}^{-1}$.

We would like to thank an anonymous referee for constructive comments and suggestions.

REFERENCES

- Abt, H. A. 1983, *ARA&A*, 21, 343
 Abt, H. A., & Levy, S. G. 1976, *ApJS*, 30, 273
 ———. 1978, *ApJS*, 36, 241
 Bhat, C. L., Houston, B. P., Issa, M. R., Mayer, C. J., & Wolfendale, A. W. 1985, *Nature*, 314, 511
 Bisiacchi, G. F., Firmani, C., & Samiento, A. F. 1983, *A&A*, 119, 167
 Blaauw, A. 1985, in *Birth and Evolution of Massive Stars*, ed. W. Boland & H. van Woerden (Dordrecht: Reidel), 211
 Bohigas, J. 1988, *A&A*, 205, 257
 Bronfman, L., Cohen, R. S., Alvarez, H., May, J., & Thaddeus, P. 1988, *ApJ*, 324, 248
 Buonanno, R., Corsi, C. E., & Fusi Pecci, F. 1989, *A&A*, 216, 80
 Burton, W. B., & Gordon, M. A. 1978, *A&A*, 63, 7
 Carlberg, R. G., Dawson, P. C., Hsu, T., & Vandenberg, D. A. 1985, *ApJ*, 294, 674
 Caswell, J. L., & Lerche, I. 1979, *MNRAS*, 187, 201
 Cester, B., Ferluga, S., & Boehm, C. 1983, *Ap&SS*, 96, 125
 D'Antona, F. 1990, in *Physical Process in Fragmentation and Star Formation*, ed. R. Capuzzo-Dolcetta, C. Chiosi, & A. Di Fazio (Dordrecht: Kluwer), 367
 D'Antona, F., & Mazzitelli, I. 1986, *A&A*, 162, 80
 Duquenoey, A. 1988, in *IAU Colloq. 96, Few Body Problems*, ed. M. J. Valtonen (Dordrecht: Kluwer), 257
 Duquenoey, A., & Mayor, M. 1989, in *Proc. of the XI European Regional Astronomy Meeting of the IAU*, ed. M. Vazquez (Cambridge: Cambridge Univ. Press)
 Ferrini, F., Palla, F., & Penco, U. 1990, in *Physical Process in Fragmentation and Star Formation*, ed. R. Capuzzo-Dolcetta, C. Chiosi, & A. Di Fazio (Dordrecht: Kluwer), 357
 Garmany, C. D., & Conti, P. S. 1988, in *IAU Symp. 88, Close Binary Stars Observations and Interpretation*, ed. M. J. Plavec, D. M. Popper, & R. K. Ulrich (Dordrecht: Reidel), 163
 Garmany, C. D., Conti, P. S., & Chiosi, C. 1982, *ApJ*, 263, 777
 Garmany, C. D., Conti, P. S., & Maasey, P. 1980, *ApJ*, 242, 1063
 Gilmore, G., Reid, N., & Hewett, P. 1985, *MNRAS*, 213, 257
 Gould, A. 1990, *MNRAS*, 244, 25
 Grenier, S., Gomez, A. E., Jaschek, C., Jaschek, M., & Hech, A. 1985, *A&A*, 145, 331
 Grennon, M. 1989, in *5th IAP Meeting Proceedings Astrophysical Ages and Dating Methods*, preprint
 Halbwachs, J. L. 1986, *A&A*, 168, 161
 ———. 1987, *A&A*, 183, 234
 Humphreys, R. M., & McElroy, D. B. 1984, *ApJ*, 284, 565
 Kuijken, K., & Gilmore, G. 1991, *ApJ*, 367, L9
 Larson, R. B. 1986, *MNRAS*, 218, 409
 Li, T. P., Riley, P. A., & Wolfendale, A. W. 1982, *J. Phys. G*, 8, 141
 Liebert, J., & Probst, R. 1987, *ARA&A*, 25, 473
 Lucy, L. B., & Ricco, E. 1979, *AJ*, 84, 401
 Maeder, A. 1990, *A&AS*, 84, 139
 Maeder, A., & Meynet, G. 1989, *A&A*, 210, 155
 Malaney, R. A., Mathew, G. J., & Dearborn, D. S. P. 1989, *ApJ*, 345, 169
 Meyer, B. S., & Schramm, D. N. 1986, *ApJ*, 311, 406
 Miller, G. E., & Scalo, J. M. 1979, *ApJS*, 41, 513
 Narayan, R. 1986, in *IAU Symp. 125, The Origin and Evolution of Neutron Stars*, ed. D. J. Helfand (Dordrecht: Reidel), 67
 Pisunukov, A. E., & Malkov, O. Yu. 1987, *Publ. Astron. Inst. Czech. Acad. Sci.*, 69, 87
 Popper, D. M. 1980, *ARA&A*, 18, 115
 Poveda, A. 1988, *Ap&SS*, 142, 67
 Rana, N. C. 1987a, *A&A*, 184, 104
 ———. 1989, in *IAU Coll. 114, White Dwarfs*, ed. W. Wegener (Dordrecht: Kluwer), 151
 ———. 1990a, in *Physical Processes in Fragmentation and Star Formation*, ed. R. Capuzzo-Dolcetta, C. Chiosi, & A. Di Fazio (Dordrecht: Kluwer), 381
 ———. 1990b, *Ap&SS*, 163, 229
 ———. 1991, *ARA&A*, 29, 129
 Reid, N., & Gilmore, G. 1982, *MNRAS*, 201, 73
 Robin, A., & Cr ez e, M. 1986, *A&A*, 157, 71
 Salpeter, E. E. 1985, *ApJ*, 121, 161
 Scalo, J. M. 1986, *Fund. Cosmic Phys.*, 11, 1
 Shu, F. H., & Lubow, S. H. 1981, *ARA&A*, 19, 277
 Smith, L. F., Biermann, P., & Mezger, P. G. 1978, *A&A*, 66, 65
 Stobie, R. S., Ishida, K., & Peacock, J. A. 1989, *MNRAS*, 238, 709
 Talbot, R. J. 1980, *ApJ*, 235, 821
 Tosi, M. 1988, *A&A*, 197, 33
 Tosi, M., & Diaz, A. I. 1985, *MNRAS*, 217, 571
 Trimble, V. 1974, *AJ*, 79, 967
 ———. 1978, *Observatory*, 98, 163
 ———. 1987, *Astron. Nach.*, 308, 343
 Trimble, V., & Walker, D. 1986, *Ap&SS*, 126, 243
 Twarog, B. A. 1980, *ApJ*, 242, 242
 Vanbeveren, D. 1984, *A&A*, 139, 545
 Van Buren, D. 1985, *ApJ*, 294, 567
 Van den Bergh, S., McClure, R. D., & Evans, R. 1987, *ApJ*, 323, 44
 Vilumsen, J. V. 1985, *ApJ*, 290, 75
 Wielen, R. 1977, *A&A*, 60, 263
 Wielen, R., & Fuchs, B. 1983, in *Kinematics, Dynamics and the Structure of the Milky Way*, ed. W. L. H. Shuter (Dordrecht: Reidel), 81
 Wolff, S. C. 1978, *ApJ*, 222, 553
 Wood, D. O. S., & Churwell, E. 1989, *ApJ*, 340, 265